

RESEARCH

Open Access



# Huangqi decoction ameliorates kidney injury in db/db mice by regulating the BMP/Smad signaling pathway

Ying Chen<sup>1</sup>, Rong Rui<sup>1</sup>, Li Wang<sup>1</sup>, Hao Wang<sup>1</sup>, Bingbing Zhu<sup>1\*</sup> and Aili Cao<sup>2\*</sup> 

## Abstract

**Purpose** This study aims to investigate the mechanism underlying the beneficial effects of Huangqi decoction (HQD) on Diabetic kidney disease (DKD) in diabetic db/db mice.

**Methods** Eight-week-old male diabetic db/db mice were randomly divided into four groups: Model (1% CMC), HQD-L (0.12 g/kg), HQD-M (0.36 g/kg), and HQD-H (1.08 g/kg) groups. Non-diabetic db/m mice were served as the control group. These mice received HQD treatment for 8 weeks. After treatment, the kidney function, histopathology, micro-assay, and protein expression levels were assessed.

**Results** HQD treatment improved the albumin/creatinine ratio (ACR) and 24 h urinary albumin excretion, prevented the pathological phenotypes of increased glomerular volume, widened mesangial areas, the of mesangial matrix proliferation, foot process effacement, decreased nephrin expression and reduced number of podocytes. Expression profiling analysis revealed global transcriptional changes that predicted related functions, diseases and pathways. HQD treatment activated protein expressions of BMP2, BMP7, BMPR2, and active-Rap1, while inhibiting Smad1 and phospho-ERK. In addition, HQD was associated with improvements in lipid deposition in the kidneys of db/db mice.

**Conclusion** HQD ameliorated the progression of DKD in db/db mice by regulating BMP transcription and downstream targets, inhibiting the phosphorylation of ERK and the expression of Smad1, promoting Rap1 binding to GTP, and regulating the lipid metabolism. These findings provide a potential therapeutic approach for treating DKD.

**Keywords** Huangqi decoction (HQD), Diabetic kidney disease (DKD), Lipid metabolism, Db/db mice

## Background

Diabetes mellitus is a common disease that affects more than 463 million adults globally [1]. Diabetic kidney disease (DKD) is one of the most common and serious chronic microvascular complications of diabetes mellitus and the main cause of end-stage renal disease (ESRD) and death. Early diagnosis of DKD is critical, as the onset of proteinuria increases the risk of progression to ESRD by approximately 14 times [2]. Although angiotensin-converting enzyme inhibitors (ACEIs) and angiotensin receptor blockers (ARBs) are commonly used in the clinical treatment of DKD, they can have adverse effects such as heart failure [3, 4]. There is a pressing need for

\*Correspondence:

Bingbing Zhu  
zbb630@126.com  
Aili Cao  
caoailli0312@sina.cn

<sup>1</sup> Department of Nephrology, Laboratory of Renal Disease, Putuo Hospital, Shanghai University of Traditional Chinese Medicine, 164 LanXi Road, Shanghai 200062, China

<sup>2</sup> Department of Nephrology, Shanghai Sixth People's Hospital Affiliated to Shanghai Jiao Tong University School of Medicine, Shanghai 200233, China



© The Author(s) 2023. **Open Access** This article is licensed under a Creative Commons Attribution 4.0 International License, which permits use, sharing, adaptation, distribution and reproduction in any medium or format, as long as you give appropriate credit to the original author(s) and the source, provide a link to the Creative Commons licence, and indicate if changes were made. The images or other third party material in this article are included in the article's Creative Commons licence, unless indicated otherwise in a credit line to the material. If material is not included in the article's Creative Commons licence and your intended use is not permitted by statutory regulation or exceeds the permitted use, you will need to obtain permission directly from the copyright holder. To view a copy of this licence, visit <http://creativecommons.org/licenses/by/4.0/>. The Creative Commons Public Domain Dedication waiver (<http://creativecommons.org/publicdomain/zero/1.0/>) applies to the data made available in this article, unless otherwise stated in a credit line to the data.

systematic approaches to improve the treatment of DKD. In addition to conventional therapeutic measures and basic recommendations, such as lifestyle changes, phytotherapy, an alternative branch of medicine, has emerged as a promising tool to support the management of diabetes mellitus and related disorders [5]. Evidence-based studies have shown that active compounds found in plant-based raw materials possess antioxidant, anti-inflammatory, and immunomodulatory properties, making them potentially beneficial in the treatment of DKD [4, 6].

Bone morphogenetic proteins (BMPs) is a member of the transforming growth factor (TGF- $\beta$ ) superfamily, known for its highly conserved functional protein. It was first discovered by Urist from a decalcified bone matrix extract and named BMP due to its ability to induce ectopic bone formation [7, 8]. Current studies have shown that BMP has a wide range of biological functions [9] and plays an instrumental role in kidney development [10]. There are two types of BMP-induced signaling pathways, including the canonical Smad-dependent pathway and Smad-independent pathways [11]. Disruption of the classic Smad-dependent BMP pathway has been linked to accelerated onset and progression of renal fibrosis [12], highlighting the significance of BMP in kidney health.

The Ras-like small GTPase Rap1 functions as a molecular switch by binding GTP or GDP to switch between active and inactivated states. The integrity of the slit diaphragm is directly linked to Rap1 signaling [13]. Previous research has revealed that abnormalities in Rap1GTP in podocytes result in variations in downstream mitogen-activated protein kinase (MAPK) signaling [14]. Furthermore, a recent study has discovered a novel mechanism in pulmonary artery smooth muscle cells, where extracellular regulated protein kinase (ERK), a component of MAPK, can regulate the phosphorylation of Smad, thereby facilitating the entry of BMP into the nucleus [15]. Notably, the activity of Rap1GTP is inversely correlated with the phosphorylation level of

ERK [14], suggesting that ERK-mediated downregulation of Rap1GTP activity may play a role in this process.

In most cases, disruptions in lipid metabolism are commonly observed in patients with DKD, and emerging research suggests that BMPs are involved in maintaining metabolic processes [16–19]. Traditional Chinese medicine (TCM), which has been widely used in China for thousands of years. One such TCM formula, Huangqi decoction (HQD), composed of Astragali Radix, Poria, Trichosanthis Radix, Ophiopogonis Radix, Schisandrae Chinensis Fructus, Glycyrrhizae Radix et Rhizoma Praeparata Cum Melle, and Rehmanniae Radix, has shown promising results in regulating DKD through multiple targets and pathways. HQD has been found to inhibit podocyte injury by modulating oxidative stress, endoplasmic reticulum stress, as well as increasing insulin sensitivity, ultimately alleviating DKD [20–25]. These studies found that Astragaloside, one of the main components of HQD, ameliorates DKD and inhibits interstitial renal fibrosis by alleviating endoplasmic reticulum stress [21]. The present investigation aims to further elucidate the mechanism by which HQD protects against renal glomerular dysfunction in DKD, providing novel insights for the treatment of DKD.

## Methods and materials

### HQD preparation

HQD, consisting of Astragali Radix, Poria, Trichosanthis Radix, Ophiopogonis Radix, Schisandrae Chinensis Fructus, Glycyrrhizae Radix et Rhizoma Praeparata Cum Melle, and Rehmanniae Radix (Table 1), were purchased from Shanghai Huayu Chinese Herbs Co. Ltd. (Shanghai, China). All the herbs were powdered and mixed thoroughly to create a homogenous mixture. The medicinal herb mixture was then subjected to triple extraction using four times volumes of water. The resulting extract was concentrated under vacuum to obtain a thick decoction. Ethanol was added to the concentrated decoction to achieve a final ethanol concentration of 70%. After

**Table 1** Huangqi Decoction composition

Chinese name	English name	Botanical name	Family	Weight (g)	Part used
Huangqi	Astragali Radix	<i>Astragalus membranaceus</i> (Fisch.) Bge. var. <i>mongholicus</i> (Bge.) Hsiao	Leguminosae	30	Root
Fuling	Poria	<i>Poria cocos</i> (Schw.) Wolf	Polyporaceae	30	Sclerotia
Tianhuafen	Trichosanthis Radix	<i>Trichosanthes kirilowii</i> Maxim	Cucurbitaceae	30	Root
Maidong	Ophiopogonis Radix	<i>Ophiopogon japonicus</i> (L.f) Ker-Gawl	Liliaceae	30	Tuber
Wuweizi	Schisandrae Chinensis Fructus	<i>Schisandra chinensis</i> (Turcz.) Baill	Magnoliaceae	15	Fruit
Zhigancao	Glycyrrhizae Radix et Rhizoma Praeparata Cum Melle	<i>Glycyrrhiza uralensis</i> Fisch	Leguminosae	15	Root and Rhizome
Dihuang	Rehmanniae Radix	<i>Rehmannia glutinosa</i> Libosch	Scrophulariaceae	45	Root

overnight precipitation, the supernatant was collected and dried in an oven at 105 °C for 48 h, resulting in a production rate of 13.3%. HQD was formulated as suspensions in 1% sodium carboxymethylcellulose in ddH<sub>2</sub>O at concentrations of 10, 40, and 110 mg/ml for use in animal studies. Intra-gastric administration was carried out at doses of 0.12, 0.36, and 1.08 g/kg, respectively.

#### Identification of the main compounds in HQD

The HQD extract was subjected to comprehensive analysis using LC–MS, following established protocols [26]. The composition of the complete HQD was thoroughly investigated, and the results are presented in the supplementary Figure S2, along with detailed MS/MS analysis elucidating the molecular characteristics of the components identified.

#### Animal treatment

All animal protocols in this study were approved by the Ethics Committee of Shanghai University of Traditional Chinese Medicine, and the animal ethics number is PZSHUTCM201225002. Db/db (C57BLKS/J-LepRdb/LepRdb) mice, also known as leptin receptor-deficient mice, are commonly used as a model to study DKD. Db/db mice spontaneously develop obesity and type 2 diabetes due to a mutation in the leptin receptor gene, which leads to insulin resistance and hyperglycemia. Db/db mice exhibit characteristics of DKD, including glomerular hypertrophy, increased urinary albumin excretion, and progressive renal fibrosis, which are known to be involved in the development and progression of DKD in humans [27–29]. In research studies involving db/db mice, db/m (C57BLKS/J-LepRdb/LepRdb/+) mice are often used as the control group. Db/m mice are typically littermates or genetically similar mice that do not carry the mutation in the leptin receptor gene, and therefore do not develop diabetes or other metabolic disorders like db/db mice. In this study, diabetic db/db mice and nondiabetic db/m control mice at the age of 6 weeks were purchased from the Nanjing Institute of Biomedicine affiliated with Nanjing University (Nanjing, China). Animals were housed in a specific-pathogen-free room in a 12:12 h light–dark cycle and were given free access to water and chow. All the operations and experimental procedures complied with the ethical standard in the Laboratory Animal Guideline for review of animal welfare, The National Standard of the People's Republic of China (GB/T 35892–2018), the Guide for the Care and Use of Laboratory Animals: Eighth Edition. After two weeks of adaptive housing and feeding, mice were randomly allocated into different groups for specific treatment. Random blood glucose levels were monitored every four weeks by blood samples obtained from the tail

vein with a glucometer (Omron HEA-230). Db/db mice were subjected to diabetes through genetic modification. Any animal that died or was severely injured during the experiment was excluded from the study. A total of diabetic db/db mice were divided into 4 groups (n = 5–6) and were administered either a vehicle (1% sodium carboxymethylcellulose, CMC) as a control, or three different doses of HQD (high dose 1.08 g/kg, medium dose: 0.36 g/kg, low dose: 0.12 g/kg). Additionally, a group of non-diabetic db/m mice received the vehicle. HQD or vehicle was administered to the animals daily in the morning via gavage for 8 consecutive weeks. Urine samples were collected from all mice at the ages of 8, 12, and 16 weeks to measure urinary protein levels. On the last day of week 16, the animals were anesthetized with an intraperitoneal injection of sodium pentobarbital (100 mg/kg) in the morning after overnight fasting and sacrificed to harvest tissues. The left kidney was divided into three parts, one part was subsequently placed into 4% paraformaldehyde for immunohistochemical stains, another part was stored in 2.5% glutaraldehyde for electron microscopy observation and the remaining part was stored in 18% sucrose at 4 °C for immunofluorescence staining. The cortex of the right kidney was stored at -80 °C for protein expression detection.

#### Urine albumin and creatinine measurement

Twenty-four-hour urine collections were obtained from mice using metabolic cages to ensure time collection. Urine albumin was measured using an ELISA kit (Bethyl Laboratory, Houston, TX), while urine creatinine was quantified using a colorimetric assay kit (Cayman Chemical, Ann Arbor, MI, USA). albumin-creatinine ratio was expressed as ACR, a widely accepted indicator of kidney function. The reproducibility of this assay was assessed, and the coefficients of variance (CV) were found to be consistently less than 3% when the same sample was measured three times consecutively, indicating high precision and accuracy in the measurements.

#### RNA isolation and micro-array analysis

Total RNA was extracted from approximately 50 mg of flash-frozen kidney cortex samples obtained from three treated and three non-treated db/db mice using the Qiazol extraction method, followed by on-column DNase I treatment (Qiagen, CA, USA). The quality of the extracted RNA was evaluated using BioAnalyzer (Agilent, CA, USA), and only samples with RNA integrity number (RIN) scores of 7 or higher were included in the subsequent analysis. Samples were sent to H-Wayen Biotechnologies (Shanghai, China) to detect the expression level of the whole genome mRNA.

### Western blot analysis

The renal cortex was homogenized in RIPA lysis buffer containing 1X protease inhibitors and phosphatase inhibitors (Beyotime, Shanghai, China), and lysates were collected after centrifugation for 10 min at 12,000 g. The concentration of total protein in the tissue lysates was determined using a BCA kit (Pierce, Rockford, IL, USA). Subsequently, 60 µg of lysate protein from each animal was separated by SDS-PAGE (8%-12%) and transferred to PVDF membranes (Millipore, IPVH00010). Then, the membranes were immunoblotted with primary antibodies against BMP2 (Abcam, Ab214821, 1:1000 dilution), BMP7 (Proteintech, 12,221-1-AP, 1:1000 dilution), BMPR2 (Proteintech, 14,376-1-AP, 1:1000 dilution), phospho-ERK (CST, 4370S, 1:2000 dilution), ERK (CST, 4695S, 1:1000 dilution), P-SMAD1,5,9 (CST, 13,820, 1:1000 dilution), SMAD4 (Affinity, AF5247, 1:500 dilution), SMAD1 (CST, 6944, 1:1000 dilution), CXCL16 (Affinity, DF13312, 1:500 dilution) and β-actin (Abcam, ab6276, 1:10,000 dilution) after blocking in 5% bovine serum albumin in TBST for 1 h. All primary antibodies were incubated at 4 °C overnight. Then membranes were washed in TBST and incubated with HRP-conjugated secondary antibody from Jackson ImmunoResearch (111-035-003 or 115-035-003) for 1 h at room temperature. To remove the residual secondary antibody, the membranes were washed in TBST and incubated with enhanced chemiluminescence (ECL) from Millipore (WBULS0500). An Image Quant LAS 500 was employed to visualize and capture the blot bands, which were quantified by densitometry using ImageJ.

### Active Rap1 pull down

The assessment of active Rap1 levels in kidney cortex was conducted using a pull-down assay, which involved the use of GST-tagged fusion proteins. These fusion proteins were designed to encompass amino acids 788–884 of the human RalGDS-RAP-binding structural domain, and were immobilized on glutathione agarose beads. The pull-down assay was performed utilizing the Active Rap1 Pull-down and Detection Kit (ThermoFisher Scientific, MA, USA).

### Immunofluorescence staining

Kidney tissues were preserved in 18% sucrose and subsequently embedded in optimum cutting temperature compound (OCT). A 4-µm section of tissue was mounted on a slide and blocked with 10% normal goat serum for 1 h at room temperature to avoid nonspecific binding. The slides were then incubated with primary antibody (WT-1, Abcam, ab89901, 1:50 dilution) at 4 °C overnight. Afterward, the slides were treated with Alexa Fluor 488-conjugated goat anti-rabbit antibody (Abcam, ab150077,

1:200 dilution) as the secondary antibody. To minimize background fluorescence, anti-fluorescence quenching blockers (Beyotime, Shanghai, P0126) were applied and coverslips were mounted. Finally, the slides were visualized using laser scanning confocal microscopy (LSM) to obtain detailed fluorescence images.

### Periodic Acid-Schiff (PAS) Staining and immunohistochemistry

Kidney tissues were fixed in 4% paraformaldehyde for 24 h, followed by dehydration, and embedded in paraffin. Paraffin sections of 4 µm thickness were cut, and PAS staining was performed according to the instructions provided in the commercial kit (Baso, Zhuhai, BA4080A). For semi-quantitative analysis, 20 glomeruli were randomly selected from each mouse kidney section under a 400× microscope, and the PAS-positive material (thylakoid matrix) was identified by the purple-red color, while the nucleus was stained blue. Image-J 2.0 image analysis software was utilized to measure the area of the thylakoid matrix and the total glomerular area. The thylakoid stroma index was calculated as thylakoid stroma area/glomerular area × 100%. Immunohistochemistry for nephrin (Abcam, ab216341, 1:500 dilution) and CXCL16 (Invitrogen, PA5-115,068, 1:100 dilution) on renal sections was performed with streptavidin–biotin peroxidase (SP) kit (ZSGB-BIO, Beijing, China) following standard protocols.

### Transmission electron microscopy

After removing the mouse kidney, the cortical portion of the kidney was meticulously sliced into thin sections measuring about 2 mm<sup>3</sup>. These sections were promptly submerged in a 2.5% glutaraldehyde electron microscope fixative solution and sent to Electron Microscope Center of Shanghai Medical College, Fudan University.

### Oil red O staining

The oil red O staining procedure for frozen sections of kidneys were immersed in oil red O solution (Oil Red O staining kit; ab150678) for 8 min, followed by incubation in 85% propylene glycol for 1 min to fix the staining. Then, the slides were rinsed with distilled water to remove excess staining and incubated twice in hematoxylin for 2 min to counterstain the nuclei. After gentle rinsing with tap water and distilled water, coverslips were mounted using glycerol to preserve the stained sections.

### Statistics analysis

The experimental results are presented as the means ± Standard error means (SEMs). Statistical analysis was performed with GraphPad Prism software 9 (GraphPad Software Inc., San Diego, CA, USA). Normality of

data was assessed using the Shapiro–Wilk test. Two-way analysis of variance (ANOVA) with Tukey's multiple comparisons and Geisser–Greenhouse correction, as well as One-way ANOVA followed by the Tukey's post hoc analysis, were employed to determine the statistical significance among groups. A significance level of  $P < 0.05$  was used to indicate statistically significant.

## Results

### HQD reduced the ACR and urinary protein levels in db/db mice

ACR and urinary albumin levels are highly sensitive indicators for early detection of kidney injury in chronic kidney disease (CKD), and can reflect the severity of kidney damage. Throughout the experiment, ACR and 24-h urinary protein levels in the db/m group remained stable. However, at 8 weeks of age, a significant increase in these two indicators was observed in the db/db group ( $P < 0.01$ , Fig. 1), indicating successful construction of the DKD model. At 12 weeks of age, although ACR and proteinuria levels were still higher in the HQD group compared to the db/m group, they were significantly lower than those in the db/db group, and this difference became more pronounced at 16 weeks of age ( $P < 0.01$ , Fig. 1A and B). Random blood glucose levels in the db/db mice continued to increase and were significantly higher than those in the non-diabetic db/m control mice. However, after treatment with different doses of HQD for 8 weeks, there was a trend of downregulation, although it did not reach statistical significance (Figure S1).

### HQD attenuates renal pathological damage and ultrastructural changes in db/db mice

To observe the effect of HQD on renal pathological injuries in db/db mice, PAS staining was performed on paraffin sections of mouse kidney tissue, and the renal pathological conditions of each group were observed by a light microscope. The results showed that compared with db/m mice, db/db mice presented with a significantly increased glomerular volume, widened mesangial areas, and increased proliferation of the mesangial matrix ( $P < 0.01$ ). After treatment with HQD, the above pathological changes were significantly improved ( $P < 0.01$ ,  $P < 0.05$ ) (Fig. 2A, D&E), indicating that HQD could alleviate the pathological damage to kidney tissue in db/db mice. To investigate the effects of HQD on podocyte structure, transmission electron microscopy was performed (Fig. 2B). Podocytes in db/db mice showed broadening, fusion, the disappearance of foot processes, a decrease in the density and number of podocytes, and thickening of the basement membrane. After treatment with HQD, the above phenomena were reduced. A decrease in nephrin (biomarker of podocyte)

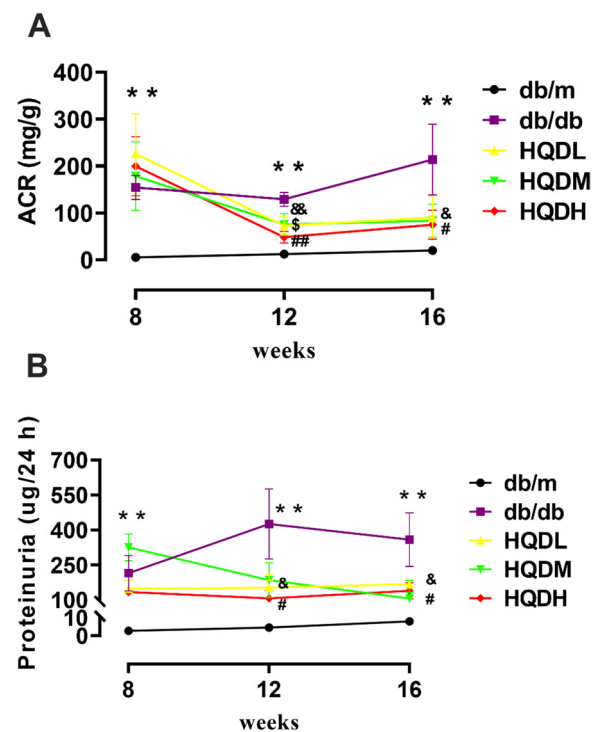


**Fig. 1** HQD reduced ACR and urinary protein levels in db/db mice. **A.** The level of urine ACR; **B.** 24-h urine protein level. Values are mean  $\pm$  SEM ( $n = 5-6$ ), \*\* $P < 0.01$  vs. db/m group; & $P < 0.05$  && $P < 0.01$  HQDL vs. db/db group, \$  $P < 0.05$  HQDM vs. db/db group, ## $P < 0.05$  ### $P < 0.01$ , HQDH vs. db/db group by two-way ANOVA with Tukey's multiple comparisons and Geisser–Greenhouse correction analysis

of glomerulus were observed in model group, which was alleviated in HQD group (Fig. 2C). These results indicate that HQD could maintain the stability of podocyte structure and change the pathological damage to podocytes.

### HQD restored the number of glomerular podocytes in db/db mice

In addition to the pathological changes, the loss of glomerular podocytes was also observed, which is known to contribute to the development of DKD. WT1, a podocyte-specific marker, was used to test whether podocyte loss occurs in db/db mice (Fig. 3). As shown in Fig. 3, the number of podocytes was downregulated in db/db mice compared with that in db/m mice, and it was upregulated in HQD-treated db/db mice compared with that in db/db mice ( $P < 0.01$ ,  $P < 0.05$ ).

### Transcriptome study of HQD in db/db mice

To further elucidate the underlying mechanism by which HQD exerts its reno-protective effects, micro-array experiments comparing HQD treated db/db mice or non-treated db/db mice. With fold changes (FC)  $\geq 2$  or  $\leq 0.5$  ( $P < 0.05$ ) as the screening criteria, 87 differentially

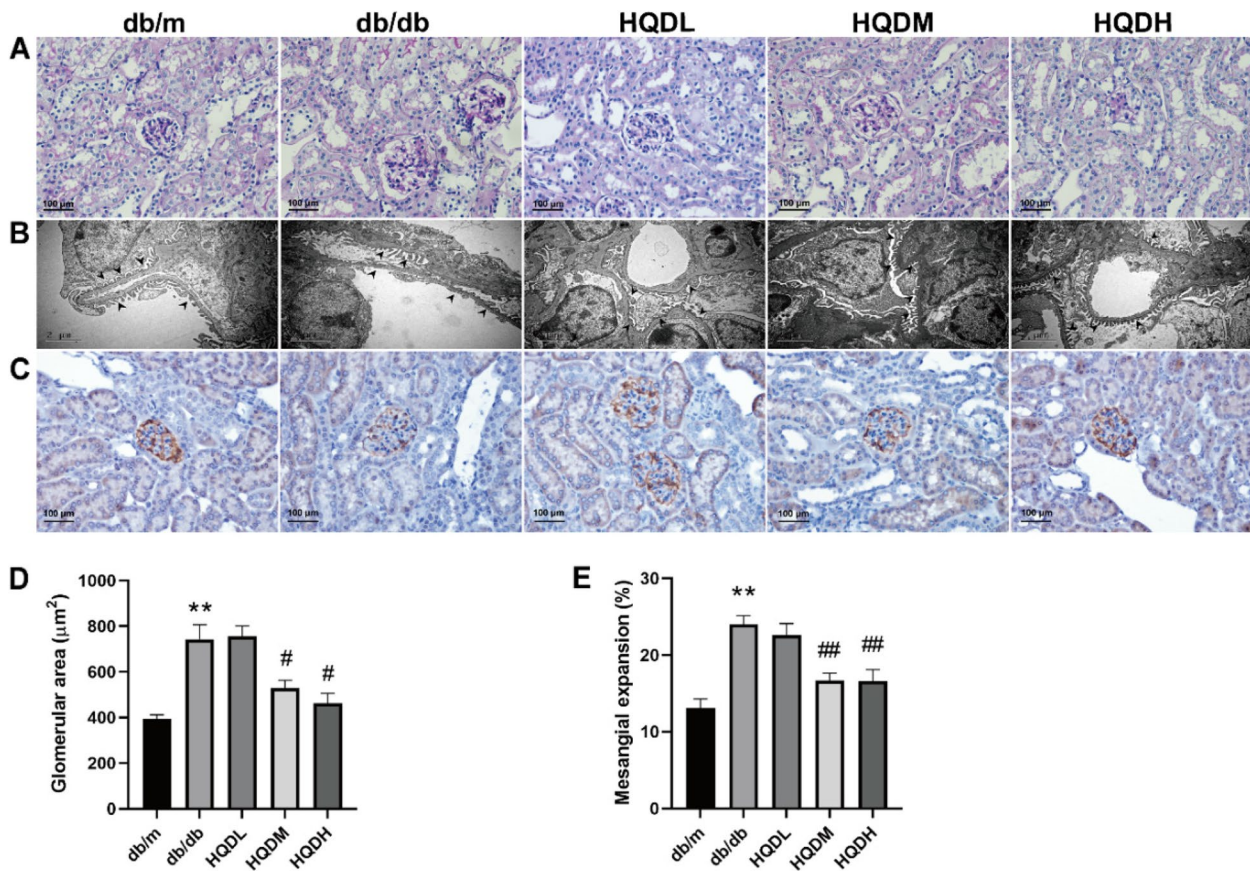


**Fig. 2** HQD attenuates renal pathological damage and ultrastructural changes in db/db mice. **A.** PAS staining; **B.** SEM images. **C.** Nephrin stained by immunohistochemistry, scale bar, 100 µm; **D.** Glomerular area (µm<sup>2</sup>). **E.** Mesangial expansion (%). Values are mean ± SEM (n = 5–6), \*\*P < 0.01 vs. db/m, #P < 0.05, ##P < 0.01 vs. db/db by one-way ANOVA with Tukey’s post doc analysis

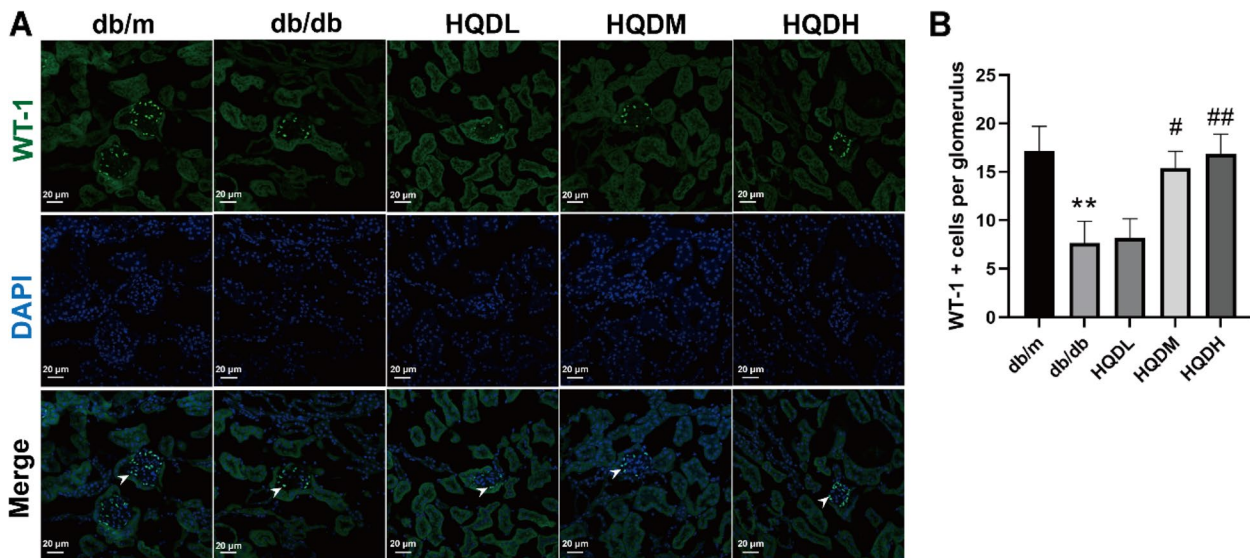


**Fig. 3** HQD restored the number of glomerular podocytes in db/db mice. **A.** Immunofluorescence shows that the reduced amount of WT-1 in db/db kidneys is significantly restored by HQD. **B.** Statistical results of the number of WT-1 positive cells, Values are mean ± SEM (n = 5–6), \*\*P < 0.01 vs. db/m, #P < 0.05, ##P < 0.01 vs. db/db by one-way ANOVA with Tukey’s post doc analysis

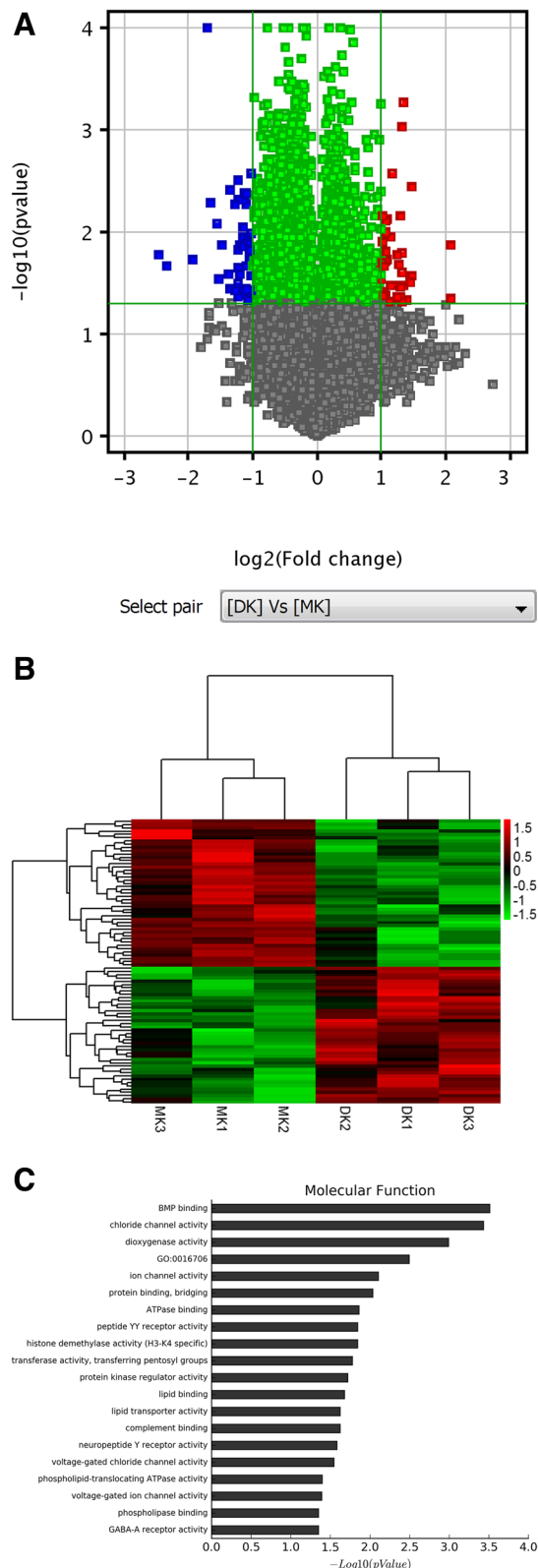


**Fig. 4** Gene expression profiling Analysis. **A.** Volcano map of differentially expressed mRNAs ( $n=3$ ). **B.** Cluster heatmap of differentially expressed mRNAs. **C.** The molecular function of differentially expressed mRNAs

expressed mRNA were obtained, 42 of which in HQD-treated samples were upregulated and 45 were downregulated. Figure 4A is the volcano map of the differentially expressed mRNA. The differentially expressed mRNA was shown in cluster heat map (Fig. 4B). Molecular function of Gene Ontology (GO) enrichment analysis showed that HQD had the greatest effect on the BMP signaling pathway (Fig. 4C).

#### HQD restored the expression levels of BMP2, BMP7, and BMPR2

In order to verify the regulatory effect of HQD, the protein expression levels of the BMP family members were detected by Western blot (Fig. 5). Compared with the db/m mice, BMP2 and BMP7 protein expression levels dropped significantly, whereas the expression levels were markedly higher after HQD treatment ( $P<0.05$ ,  $P<0.01$ ) (Figs. 5A and B). Further observation showed that HQD could significantly upregulate BMPR2 expression ( $P<0.05$ ,  $P<0.01$ ) (Figs. 5A and B). These findings suggest that HQD might play a protective role in the kidneys of db/db mice by regulating BMPR2 and promoting BMP transport.

#### HQD downregulated the expression of the Smad protein in the kidneys of db/db mice

In order to further explore the mechanism by which HQD may restore the levels of BMPs, the expression of Smad proteins was investigated. Smad1 was significantly increased in the kidneys of db/db mice, and HQD intervention appreciably inhibited its expression ( $P<0.05$ , Fig. 6). Notably, there was no significant change in the expression of Smad4, indicating that HQD primarily affects BMP signal transduction through Smad1 rather than Smad4.

#### HQD downregulated the expression of ERK and promoted Rap1 binding to GTP

Subsequently, the phosphorylation status of ERK and the activity of Rap1 were assessed. The protein level of phospho-ERK in the kidneys of db/db mice was markedly increased, and its expression was effectively restored by HQD ( $P<0.05$ ,  $P<0.01$ ) (Fig. 7A&B). Rap1 acts as a molecular switch by binding GDP and GTP to switch between its inactive and activated states. The activity of Rap1 was significantly decreased in db/db mice, while HQD treatment restored the expression of Rap1-GTP

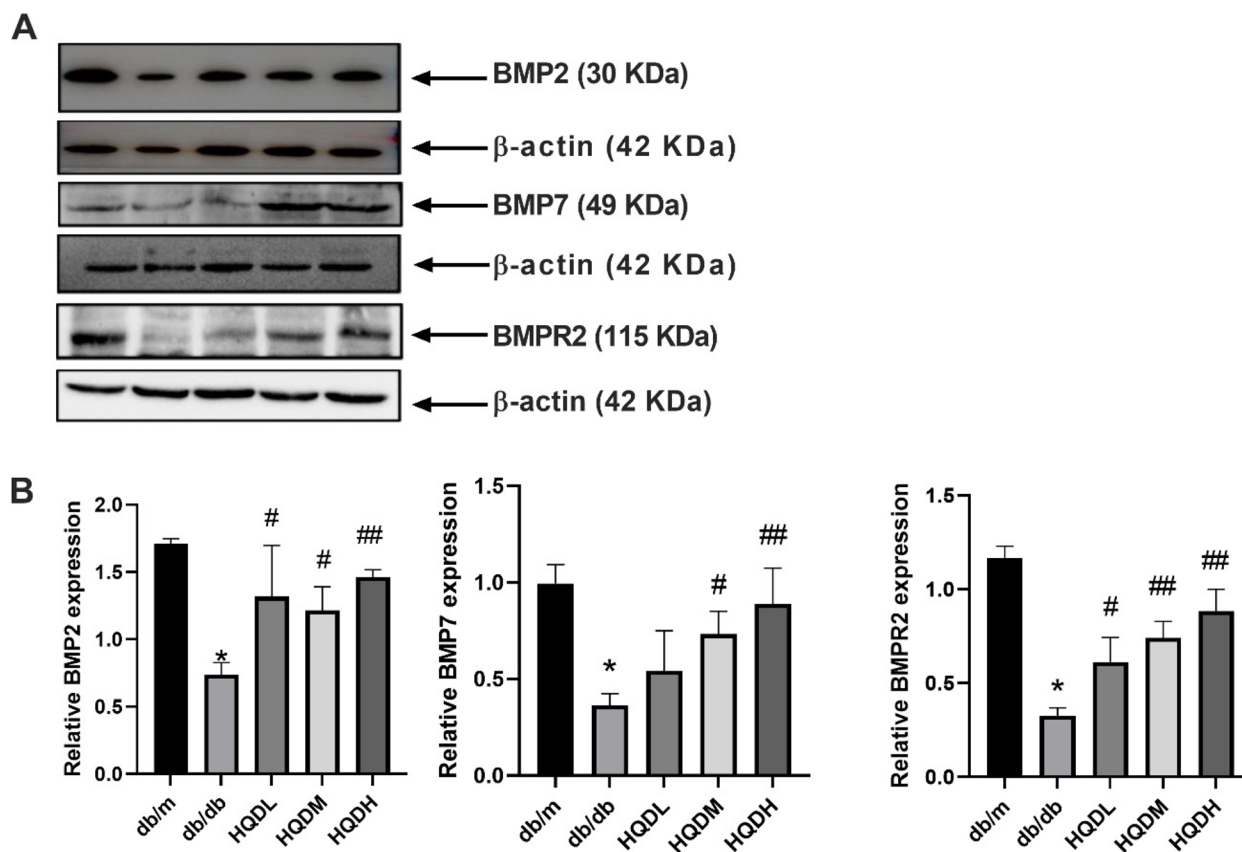


**Fig. 5** HQD restored the expression levels of BMP2, BMP7, and BMPR2. **A.B.** Western blot analysis of renal cortical BMP2, BMP7, and BMPR2 expression levels. Values are mean  $\pm$  SEM (n = 3) \* $P$  < 0.05 vs. db/m, # $P$  < 0.05, ## $P$  < 0.01 vs. db/db by one-way ANOVA with Tukey's post hoc analysis

in the kidneys of db/db mice to normal levels ( $P$  < 0.05, Fig. 7C&D).

#### HQD ameliorates lipid metabolism disorders in db/db mice

Diabetes mellitus is a disease characterized by metabolic abnormalities. Prolonged hyperglycemia associated with diabetes eventually leads to lipid metabolism disorders. In this study, it was observed that HQD significantly improved renal lipid deposition in db/db mice, as evidenced by Oil Red O staining (Fig. 8A). CXCL16, a key intermediate mediator of lipid accumulation, localizes in both tubules and glomeruli. In diabetic mice, the intensity of CXCL16 staining in glomerular was significantly increased. However, HQD dose-dependently decreased the expression of CXCL16 in both glomeruli and tubules (Fig. 8B). Western blots analysis further confirmed these findings ( $P$  < 0.05, Fig. 8C&D).

#### Discussion

DKD is one of the most devastating and prevalent chronic microvascular complications of diabetes and a major contributor to ESRD and death. Experimental

studies have demonstrated that TCM can effectively improve DKD [30, 31], but the relevant pharmacological mechanisms underlying these effects are not sufficiently understood. The formulation of HQD has been supported by years of clinical and basic research, confirming its suitability and reliability in protecting against CKD [20, 21, 23, 24]. In this study, the therapeutic efficacy of HQD was associated with improvements of BMP/Smad signaling pathway, which is consistent with micro-assay results. Furthermore, HQD was able to regulate abnormal lipid levels that occur during long-standing chronic hyperglycemia, thus restoring lipid metabolism balance. These results suggest that HQD may be superior to many current drugs due to its multiple activities, which can potentially alleviate the clinical symptoms of DKD.

HQD treatment induces a distinct gene expression pattern that is mainly related to BMP signaling. BMPs belong to the TGF- $\beta$  superfamily, which is a class of highly conserved functional proteins. In BMP4 $^{-/-}$  transgenic mice, which lack BMP4 secretion by podocytes, pathological changes such as glomerular microaneurysms, collapsed glomerular capillaries, enlarged glomerular capsules, and



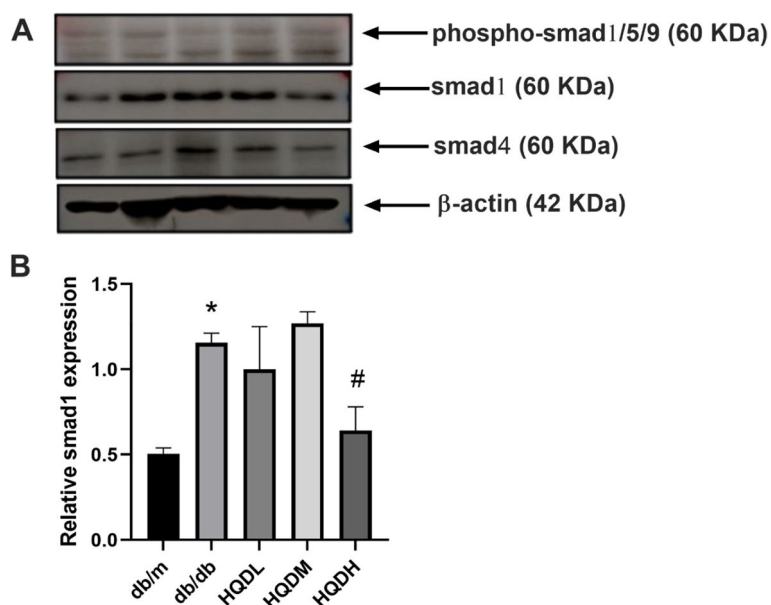


**Fig. 6** HQD downregulated the expression of the Smad1 protein in the kidneys of db/db mice. **A.** The protein expression levels of P-Smad1/5/9, Smad1 and Smad4 in the kidney cortex by Western blot assay. **B.** Statistical results of the expression level of Smad1, Values are mean ± SEM (n = 3), \*P < 0.05, compared with db/m group; ##P < 0.05, compared with db/db group. \*P < 0.05 vs. db/m, #P < 0.05 vs. db/db by one-way ANOVA with Tukey's post doc analysis

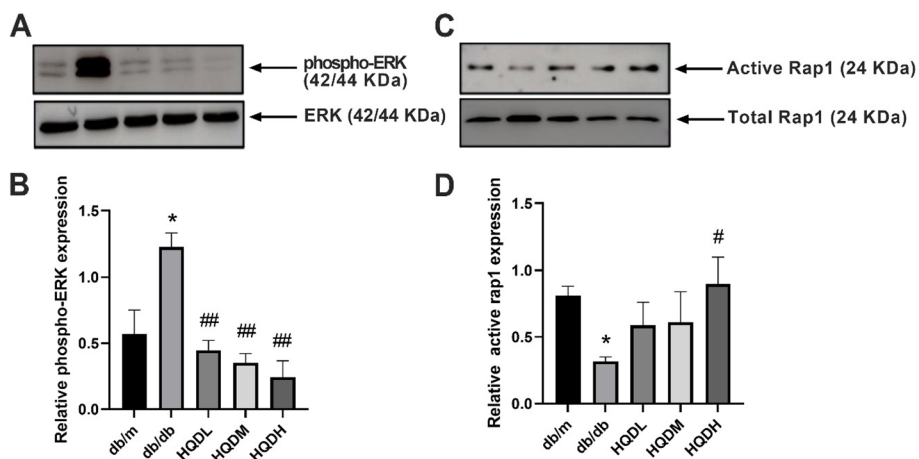


**Fig. 7** HQD downregulated the expression of ERK and promoted Rap1 binding to GTP. **A. B.** The protein expression levels of phospho-ERK in the kidney cortex by Western blot assay. **C. D.** In the kidney, the active-Rap1 protein was enriched using the active-rap1 pull-down kit, and alterations were detected by Western blot. Values are mean ± SEM (n = 3), \*P < 0.05 vs. db/m, #P < 0.05 vs. db/db by one-way ANOVA with Tukey's post doc analysis

reduced normal proximal tubules have been observed, indicating that BMP of podocyte origin has an important function in glomerular capillary formation [32]. BMP4 has also been shown to regulate the deposition of the extracellular matrix in the glomerular thylakoid region of DKD mice, which exacerbates glomerular lesions [33]. In the early formation of type I diabetes in

rats, the expression of renal BMP7 and its receptors was reduced or lost. However, pharmacological intervention has been shown to improve renal function, reduce fibronectin expression, and reverse the expression of both BMP7 and its receptor compared to DKD rats [34]. Furthermore, BMP7 has been found to protect thylakoid cells from high glucose-induced oxidative stress, thereby

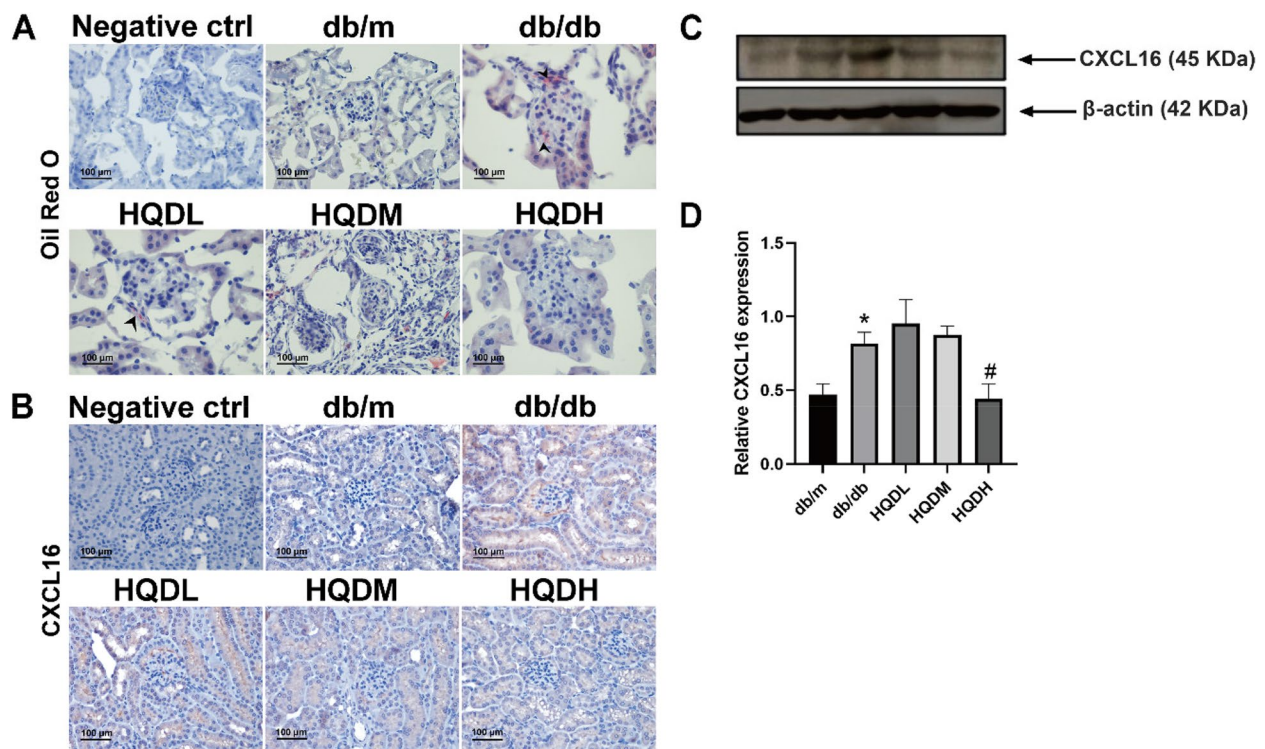


**Fig. 8** HQD ameliorates lipid metabolism disorders in db/db mice. **A.** Frozen sections of mouse kidneys were stained with Oil Red O ( $n=5$ ). **B.** IHC staining of mouse paraffin sections for CXCL16 ( $n=5$ ). **C.D** The protein expression levels of CXCL16 in the kidney cortex by Western blot assay ( $n=3$ ). \* $P < 0.05$  vs. db/m, # $P < 0.05$  vs. db/db by one-way ANOVA with Tukey's post hoc analysis

delaying DKD [35]. BMPRs are a group of serine/threonine kinase receptors with abundant cysteine extracellular structures, single-chain transmembrane regions and intracellular kinase regions. These receptors include type I and type II receptors, where type I receptors are the downstream activating components of type II receptors [36]. Gene microarray data has showed that HQD treatment in db/db mice robustly alters glomerular BMP binding pathway-related signaling. Further analysis of renal BMP-related proteins in db/db mice and discovered that HQD could effectively restore the expression levels of BMP2 and BMP7, and dramatically elevate the expression of BMPR-2. This finding suggests that HQD may protect against DKD by regulating BMPR-2 and promoting BMP2 and BMP7 transport.

BMPs are part of the kinase transduction system, where ligand-receptor binding leads to phosphorylation of the threonine-serine-rich (GS) structural domain in the cell membrane of the type I receptor by the type II receptor. This phosphorylation event activates the Smad protein, which further transduces the biological message of BMP [36]. The classic BMP pathway transduction is dependent on the modulation of Smad proteins, which are regulated by various molecular mechanisms, affecting signaling at different levels including ligands, receptors, and

signal transduction factors. Deletion of BMPR-2 inhibits the downstream Smad1/5 phosphorylation, which in turn inhibits BMP signaling [34]. Previous studies found that HQD could participate in regulating renal interstitial fibrosis through the Smad signaling pathway [21]. In the current study, it was observed that renal Smad protein expression levels were elevated in db/db mice. However, the increased expression of Smad1 protein in db/db mice was effectively suppressed by treatment with HQD. Meanwhile, HQD did not affect Smad4 expression. This discrepancy may be attributed to the fact that Smad4 is a coregulated component of the TGF- $\beta$  and BMP signaling pathways, and thus may exert opposing effects on the kidney. It has been suggested that Smad4 deficiency inhibits renal fibrosis, but it can also result in increased kidney inflammation [37].

The Ras-like small GTPase Rap1 functions as a molecular switch by binding GTP or GDP to switch between its activation and inactivation states, and the absence of Rap1 signaling is directly related to the integrity of the podocyte [38]. Additionally, ERK, a member of the MAPK family, has been shown to regulate the phosphorylation of Smad1 in pulmonary artery smooth muscle cells, leading to the promotion of BMP entry into the nucleus [39]. Interestingly, decreased phosphorylation

of ERK has been observed in the glomeruli of FSGS patients, which correlates with the inactivation of Rap1GTP [14]. However, treatment with HQD has been shown to restore the phosphorylation level of ERK and the binding of Rap1 to GTP. It's worth noting that the results may be influenced by other cells in the kidney, such as endothelial cells and mesangial cells and other resident cells, and further in vitro studies are needed to explore the relationship between ERK and Rap1 activation specifically in podocytes.

In patients with DKD, disruptions in lipid metabolism are commonly observed. BMPs are also known to be involved in maintaining metabolic processes [19], as evidenced by increased expression of BMP2 in human adipose tissue and studies in mice showing that BMP2 is associated with the production of white adipose tissue [40, 41]. Hata et al. demonstrated that BMP2 induces adipogenesis in C3H10T1/2 cells through the activation of peroxisome proliferator-activated receptor  $\gamma$  (PPAR $\gamma$ ) by the Smad and p38 MAPK signaling pathways [42]. On the other hand, BMP7 is closely associated with brown adipogenesis, and deletion of BMP7 in mice results in a significant reduction in brown adiposity at birth [43]. In a study involving obese db/db mice, intraperitoneal injection of BMP7 resulted in a distinct reduction in body weight and body fat compared to controls one month later [44]. In this study, db/db mice showed significant glomerular lipid accumulation compared to controls. HQD improved the extent of lipid accumulation in db/db mice while modulating BMP. As HQD consists of seven herbs and has multiple pathways according to its complicated components and the results of the micro-assay study. Transcriptomic analysis revealed that HQD had the greatest effect on the BMP signaling pathway. ERK, Smad1, BMPs were regulated by HQD in the kidney in db/db mice. However, further studies, such as using transgenic mice or ERK inhibitors, are needed to elucidate the key mechanism underlying the effects of HQD.

## Conclusions

In general, HQD demonstrated a significant protective effect against DKD. This beneficial effect may be attributed to several mechanisms. Firstly, HQD was found to promote the transcription of BMPs and their downstream target genes by upregulating BMPR-II expression. Moreover, HQD was shown to regulate the phosphorylation of ERK and the expression of Smad1 by promoting the binding of Rap1 to GTP, thus modulating the fibrotic signaling pathways. Furthermore, HQD was also found to have a notable role in regulating lipid metabolism dysfunction in DKD, providing a new avenue for future research on HQD. The exact mechanisms underlying this effect are not yet fully

understood, but HQD has been shown to modulate lipid metabolism-related gene expression and improve lipid profiles in animal studies, suggesting a potential role in ameliorating lipid abnormalities commonly associated with DKD.

## Abbreviations

ACEIs	Angiotensin-converting enzyme inhibitors
ACR	Albumin/creatinine ratio
ARBs	Angiotensin receptor blockers
BMPs	Bone morphogenetic proteins
CKD	Chronic kidney disease
CMC	Carboxymethylcellulose
CV	Coefficients of variance
DKD	Diabetic kidney disease
ECL	Enhanced chemiluminescence
ERK	Extracellular regulated protein kinase
ESRD	End-stage renal disease
FC	Fold changes
GO	Gene Ontology
HQD	Huangqi decoction
LSM	Laser scanning confocal microscopy
MAPK	Mitogen-activated protein kinase
OCT	Optimum cutting temperature compound
PAS	Periodic Acid-Schiff
RIN	RNA integrity number
SEMs	Standard error means
TCM	Traditional Chinese medicine
TGF- $\beta$	Transforming growth factor

## Supplementary Information

The online version contains supplementary material available at <https://doi.org/10.1186/s12906-023-04029-1>.

**Additional file 1.**

**Additional file 2.**

## Acknowledgements

Thanks to everyone who contributed to this article.

## Authors' contributions

AC and BZ conceived and designed research. YC and RR conducted experiments. LW and HW analyzed data. AC wrote the manuscript. All authors read and approved the manuscript.

## Funding

This study was funded by Shanghai Pujiang Program (21PJ1412400), Science and Technology Innovation Project of Putuo District Health System (ptk-wws202001), Shanghai University of Traditional Chinese Medicine (2020LK070) and Clinical specialty of Shanghai Putuo District Health System (2021tszk02).

## Availability of data and materials

The datasets generated during the current study are available in NCBI repository using the accession number GSE225477.

## Declarations

### Ethics approval and consent to participate

All experiments were approved by Shanghai University of Traditional Chinese Medicine Animal Care and Use Committee (PZSHUTCM201225002) and authorized by the Experimental Animal Ethics Committee of Shanghai University of Traditional Chinese Medicine. All experiments were performed in accordance with relevant guidelines and regulations. All methods are reported in accordance with ARRIVE guidelines for the reporting of animal

experiments. Plant accordance general statement: Experimental research and field studies on plants including the collection of plant material are comply with relevant guidelines and regulation.

#### Consent for publication

Not applicable.

#### Competing interests

The author(s) declare(s) that they have no competing interests.

Received: 7 February 2023 Accepted: 8 June 2023

Published online: 26 June 2023

#### References

- International Diabetes Federation, IDF Diabetes Atlas 2019 [Available from: <https://diabetesatlas.org/en/sections/worldwide-toll-of-diabetes.html>.
- Chen TK, Knicely DH, Grams ME. Chronic kidney disease diagnosis and management: a review. *JAMA*. 2019;322(13):1294–304.
- Boehm M, Crawford M, Moscovitz JE, Carpino PA. Diabetes area patent participation analysis - part II: years 2011–2016. *Expert Opin Ther Pat*. 2018;28(2):111–22.
- Sattar N, Preiss D. Research digest: progress in microvascular complications. *Lancet Diabetes Endocrinol*. 2018;6(2):93.
- Butnariu M, Fratantonio D, Herrera-Bravo J, Sukreet S, Martorell M, Ekaterina Robertovna G, et al. Plant-food-derived bioactives in managing hypertension: From current findings to upcoming effective pharmacotherapies. *Current topics in medicinal chemistry*. 2023.
- Butnariu M, Quispe C, Koirala N, Khadka S, Salgado-Castillo CM, Akram M, et al. Bioactive effects of curcumin in human immunodeficiency virus infection along with the most effective isolation techniques and type of nanoformulations. *Int J Nanomed*. 2022;17:3619–32.
- Lowery JW, Rosen V. The BMP pathway and its inhibitors in the skeleton. *Physiol Rev*. 2018;98(4):2431–52.
- Chen G, Deng C, Li YP. TGF- $\beta$  and BMP signaling in osteoblast differentiation and bone formation. *Int J Biol Sci*. 2012;8(2):272–88.
- Hiepen C, Jatzlau J, Hildebrandt S, Kampfrath B, Goktas M, Murgai A, et al. BMPR2 acts as a gatekeeper to protect endothelial cells from increased TGF $\beta$  responses and altered cell mechanics. *PLoS Biol*. 2019;17(12):e3000557.
- Weber S, Taylor JC, Winyard P, Baker KF, Sullivan-Brown J, Schild R, et al. SIX2 and BMP4 mutations associate with anomalous kidney development. *J Am Soc Nephrol*. 2008;19(5):891–903.
- Woo JK, Shin JH, Lee SH, Park HM, Cho SY, Sung YM, et al. Essential role of Ahnak in adipocyte differentiation leading to the transcriptional regulation of Bmpr1alpha expression. *Cell Death Dis*. 2018;9(9):864.
- Vigolo E, Marko L, Hinze C, Muller DN, Schmidt-Ullrich R, Schmidt-Ott KM. Canonical BMP signaling in tubular cells mediates recovery after acute kidney injury. *Kidney Int*. 2019;95(1):108–22.
- Maywald ML, Picciotto C, Lepa C, Bertgen L, Yousaf FS, Ricker A, et al. Rap1 activity is essential for focal adhesion and slit diaphragm integrity. *Front Cell Dev Biol*. 2022;10:790365.
- Zhu B, Cao A, Li J, Young J, Wong J, Ashraf S, et al. Disruption of MAGI2-RapGEF2-Rap1 signaling contributes to podocyte dysfunction in congenital nephrotic syndrome caused by mutations in MAGI2. *Kidney Int*. 2019;96(3):642–55.
- Meng XM, Huang XR, Xiao J, Chung AC, Qin W, Chen HY, et al. Disruption of Smad4 impairs TGF- $\beta$ /Smad3 and Smad7 transcriptional regulation during renal inflammation and fibrosis in vivo and in vitro. *Kidney Int*. 2012;81(3):266–79.
- Mitrofanova A, Burke G, Merscher S, Fornoni A. New insights into renal lipid dysmetabolism in diabetic kidney disease. *World J Diabetes*. 2021;12(5):524–40.
- Schelling JR. The Contribution of Lipotoxicity to Diabetic Kidney Disease. *Cells*. 2022;11(20):3236.
- Wang Y, Ma C, Sun T, Ren L. Potential roles of bone morphogenetic protein-9 in glucose and lipid homeostasis. *J Physiol Biochem*. 2020;76(4):503–12.
- Blazquez-Medela AM, Jumabay M, Bostrom KI. Beyond the bone: bone morphogenetic protein signaling in adipose tissue. *Obes Rev*. 2019;20(5):648–58.
- Jiang MQ, Wang L, Cao AL, Zhao J, Chen X, Wang YM, et al. HuangQi decoction improves renal tubulointerstitial fibrosis in mice by inhibiting the up-regulation of Wnt/ $\beta$ -Catenin signaling pathway. *Cell Physiol Biochem*. 2015;36(2):655–69.
- Zhao J, Wang L, Cao AL, Jiang MQ, Chen X, Wang Y, et al. HuangQi Decoction ameliorates renal fibrosis via TGF- $\beta$ /Smad signaling pathway in vivo and in vitro. *Cell Physiol Biochem*. 2016;38(5):1761–74.
- Han H, Cao A, Wang L, Guo H, Zang Y, Li Z, et al. Huangqi decoction ameliorates streptozotocin-induced Rat diabetic nephropathy through antioxidant and regulation of the TGF- $\beta$ /MAPK/PPAR- $\gamma$  signaling. *Cell Physiol Biochem*. 2017;42(5):1934–44.
- Chu S, Wang L, Mao XD, Peng W. Improvement of huangqi decoction on endothelial dysfunction in 5/6 nephrectomized rats. *Cell Physiol Biochem*. 2016;40(6):1354–66.
- Chen X, Wang H, Jiang M, Zhao J, Fan C, Wang Y, et al. Huangqi (astragalus) decoction ameliorates diabetic nephropathy via IRS1-PI3K-GLUT signaling pathway. *Am J Transl Res*. 2018;10(8):2491–501.
- Li Z, Deng W, Cao A, Zang Y, Wang Y, Wang H, et al. Huangqi decoction inhibits hyperglycemia-induced podocyte apoptosis by down-regulated Nox4/p53/Bax signaling in vitro and in vivo. *Am J Transl Res*. 2019;11(5):3195–212.
- Chu S, Mao XD, Wang L, Peng W. Effects of huang qi decoction on endothelial dysfunction induced by homocysteine. Evidence-based complementary and alternative medicine : eCAM. 2016;2016:7272694.
- Sharma K, McCue P, Dunn SR. Diabetic kidney disease in the db/db mouse. *Am J Physiol Renal Physiol*. 2003;284(6):F1138–44.
- Tesch GH, Lim AK. Recent insights into diabetic renal injury from the db/db mouse model of type 2 diabetic nephropathy. *Am J Physiol Renal Physiol*. 2011;300(2):F301–10.
- Allen TJ, Cooper ME, Lan HY. Use of genetic mouse models in the study of diabetic nephropathy. *Curr DiabRep*. 2004;4(6):435–40.
- Zhang L, Miao R, Yu T, Wei R, Tian F, Huang Y, et al. Comparative effectiveness of traditional Chinese medicine and angiotensin converting enzyme inhibitors, angiotensin receptor blockers, and sodium glucose cotransporter inhibitors in patients with diabetic kidney disease: a systematic review and network meta-analysis. *Pharmacol Res*. 2022;177:106111.
- Tang G, Li S, Zhang C, Chen H, Wang N, Feng Y. Clinical efficacies, underlying mechanisms and molecular targets of Chinese medicines for diabetic nephropathy treatment and management. *Acta Pharm Sin B*. 2021;11(9):2749–67.
- Ueda H, Miyazaki Y, Matsusaka T, Utsunomiya Y, Kawamura T, Hosoya T, et al. Bmp in podocytes is essential for normal glomerular capillary formation. *J Am Soc Nephrol*. 2008;19(4):685–94.
- Fujita Y, Tominaga T, Abe H, Kangawa Y, Fukushima N, Ueda O, et al. An adjustment in BMP4 function represents a treatment for diabetic nephropathy and podocyte injury. *Sci Rep*. 2018;8(1):13011.
- Wang S, de Caestecker M, Kopp J, Mitu G, Lapage J, Hirschberg R. Renal bone morphogenetic protein-7 protects against diabetic nephropathy. *J Am Soc Nephrol*. 2006;17(9):2504–12.
- Wang SN, Lapage J, Hirschberg R. Loss of tubular bone morphogenetic protein-7 in diabetic nephropathy. *J Am Soc Nephrol*. 2001;12(11):2392–9.
- Kashima R, Hata A. The role of TGF- $\beta$  superfamily signaling in neurological disorders. *Acta Biochim Biophys Sin (Shanghai)*. 2018;50(1):106–20.
- Qu X, Jiang M, Sun YB, Jiang X, Fu P, Ren Y, et al. The Smad3/Smad4/CDK9 complex promotes renal fibrosis in mice with unilateral ureteral obstruction. *Kidney Int*. 2015;88(6):1323–35.
- Potla U, Ni J, Vadaparampil J, Yang G, Leventhal JS, Campbell KN, et al. Podocyte-specific RAP1GAP expression contributes to focal segmental glomerulosclerosis-associated glomerular injury. *J Clin Invest*. 2014;124(4):1757–69.
- Yang J, Li X, Al-Lamki RS, Southwood M, Zhao J, Lever AM, et al. Smad-dependent and smad-independent induction of id1 by prostacyclin analogues inhibits proliferation of pulmonary artery smooth muscle cells in vitro and in vivo. *Circ Res*. 2010;107(2):252–62.
- Guiu-Jurado E, Unthan M, Bohler N, Kern M, Landgraf K, Dietrich A, et al. Bone morphogenetic protein 2 (BMP2) may contribute to partition of energy storage into visceral and subcutaneous fat depots. *Obesity (Silver Spring)*. 2016;24(10):2092–100.

41. Shao M, Ishibashi J, Kusminski CM, Wang QA, Hepler C, Vishvanath L, et al. Zfp423 maintains white adipocyte identity through suppression of the beige cell thermogenic gene program. *Cell Metab.* 2016;23(6):1167–84.
42. Hata K, Nishimura R, Ikeda F, Yamashita K, Matsubara T, Nokubi T, et al. Differential roles of Smad1 and p38 kinase in regulation of peroxisome proliferator-activating receptor gamma during bone morphogenetic protein 2-induced adipogenesis. *Mol Biol Cell.* 2003;14(2):545–55.
43. Tseng YH, Kokkotou E, Schulz TJ, Huang TL, Winnay JN, Taniguchi CM, et al. New role of bone morphogenetic protein 7 in brown adipogenesis and energy expenditure. *Nature.* 2008;454(7207):1000–4.
44. Chattopadhyay T, Singh RR, Gupta S, Surolia A. Bone morphogenetic protein-7 (BMP-7) augments insulin sensitivity in mice with type II diabetes mellitus by potentiating PI3K/AKT pathway. *BioFactors.* 2017;43(2):195–209.

### Publisher's Note

Springer Nature remains neutral with regard to jurisdictional claims in published maps and institutional affiliations.

Ready to submit your research? Choose BMC and benefit from:

- fast, convenient online submission
- thorough peer review by experienced researchers in your field
- rapid publication on acceptance
- support for research data, including large and complex data types
- gold Open Access which fosters wider collaboration and increased citations
- maximum visibility for your research: over 100M website views per year

At BMC, research is always in progress.

Learn more [biomedcentral.com/submissions](https://biomedcentral.com/submissions)

